

Michael Soussan  
Christophe Aubé  
Stéphane Bahrami  
Jérôme Boursier  
Dominique Charles Valla  
Valérie Vilgrain

## Incidental focal solid liver lesions: diagnostic performance of contrast-enhanced ultrasound and MR imaging

Received: 21 July 2009  
Revised: 14 November 2009  
Accepted: 20 November 2009  
Published online: 13 January 2010  
© European Society of Radiology 2009

M. Soussan · V. Vilgrain (✉)  
Department of Radiology,  
Assistance Publique des Hôpitaux  
de Paris, APHP, Hôpital Beaujon,  
100 bd du Général Leclerc,  
92110 Clichy, France  
e-mail: valerie.vilgrain@bjn.aphp.fr  
Tel.: +33-1-40875358  
Fax: +33-1-40870548

C. Aubé  
Department of Radiology,  
CHU Angers,  
Angers, France

C. Aubé  
Laboratoire HIFIH,  
UPRES 3859, IFR 132 Université,  
Angers, France

S. Bahrami  
Department of Medical Statistics,  
Assistance Publique des Hôpitaux  
de Paris, APHP,  
Université Paris-Dauphine,  
Paris, France

J. Boursier  
Department of Hepatogastroenterology  
and Laboratoire HIFIH, CHU Angers,  
UPRES 3859, IFR 132 Université,  
Angers, France

D. C. Valla · V. Vilgrain  
Université Paris7 Denis Diderot,  
75018 Paris, France

D. C. Valla · V. Vilgrain  
INSERM Centre de recherche  
Biomédicale Bichat Beaujon,  
CRB3 U773,  
75018 Paris, France

D. C. Valla  
Department of Hepatology, Assistance  
Publique des Hôpitaux de Paris, APHP,  
Hôpital Beaujon,  
Clichy, France

**Abstract Objective:** To prospectively assess the diagnostic performance of contrast-enhanced ultrasound (CEUS) and MR imaging in incidental solid focal liver lesions not characterised on ultrasound. **Materials and methods:** Forty-seven patients with 50 lesions underwent MR imaging and CEUS: 24 focal nodular hyperplasias (FNH), 11 adenomas, 10 haemangiomas, 1 focal fatty change and 4 malignant lesions were identified. Two experienced radiologists randomly reviewed contrast-enhanced MR imaging and CEUS data, and provided the most

likely diagnosis. Sensitivity (Se), specificity (Sp), likelihood ratios (LR) and kappa value were calculated. **Results:** A histotype diagnosis was obtained in 66–52% with MR imaging and 52–53% with CEUS, respectively, for both readers. Se, Sp and LR for haemangioma were 100–100, 100–100 and 78–78 with MR imaging and 89–89, 100–100 and 68–70 with CEUS; for FNH with MR imaging they were 88–63, 96–100 and 23–34 and 74–67, 88–96 and 6–17 with CEUS. If the diagnosis of haemangioma was uncertain with CEUS, MR imaging always confirmed the diagnosis. If the diagnosis of FNH was uncertain with either CEUS or MR imaging, the other imaging technique confirmed the diagnosis in approximately half the cases. **Conclusion:** Both CEUS and MR imaging have a high diagnostic performance in incidental focal liver lesions and are complementary when diagnosis is uncertain.

**Keywords** Liver neoplasms · Ultrasound · MR imaging · Liver · Diagnosis · Imaging

### Introduction

The characterisation of incidentally detected focal lesions is one of the most common and sometimes troublesome issues in liver imaging. Unsuspected lesions are frequently detected in patients who do not have chronic liver disease

nor a history of malignancy during an abdominal ultrasound examination. Most of these incidental lesions are benign [1]. While a reliable diagnosis is usually made on the basis of ultrasound findings in the case of simple cysts and haemangiomas with a typical hyperechoic appearance, lesions with non-specific ultrasound features must be

further investigated. Nowadays MR imaging is the gold standard and has a high diagnostic value for characterising haemangiomas and focal nodular hyperplasia (FNH), two lesions that most frequently cause incidental findings, with a specificity close to 100% if all diagnostic criteria are present [2, 3]. Recently, contrast-enhanced ultrasound (CEUS) has made an important diagnostic contribution to the characterisation of liver lesions. It significantly improves diagnostic results compared with baseline US [4], and the study of all the vascular phases improves diagnostic specificity [5]. Furthermore, the European Federation of Societies for Ultrasound in Medicine and Biology (EFSUMB) guidelines recommends the use of CEUS to diagnose benign focal lesions not characterised in baseline ultrasound, although these recommendations are not based on studies that have compared CEUS with other imaging techniques such as CT or MR imaging [6, 7].

Our purpose was to prospectively evaluate the sensitivities, specificities and likelihood ratios of CEUS in incidental solid liver lesions that were not completely characterised on ultrasound, compared with non-hepatospecific MR imaging. The choice of MR imaging was based on the high value of MR imaging in characterising focal liver lesions and its superiority over CT in small lesions [8, 9]. We also evaluated the interobserver agreement and a possible complementary role of both techniques.

## Materials and methods

### Study population

This prospective and bicentric study was approved by the institutional ethics review board. The two centres are referral centres for hepatobiliary diseases. All patients gave informed consent. Inclusion criteria were patients with at least one incidental solid focal liver lesion that was detected on routine US but not completely characterised, thus requiring MR imaging. All these patients underwent liver contrast-enhanced MR imaging and a liver contrast-enhanced US in the same centre at an interval of less than 1 month (median 5 days; range 0–26 days). Patients with a history of cancer, chronic liver disease or chronic hepatitis B or C infection were excluded. Patients with severe cardiac insufficiency, left to right cardiac shunts or acute coronaryopathy, and pregnant or lactating patients were also excluded.

In a 2-year period, 47 patients ( $n=32$  in centre 1;  $n=15$  in centre 2) were recruited. Fifty solid focal liver lesions were depicted in 12 men and 35 women, with a mean age of 45 (range 20–85).

### Final diagnosis

The 50 liver lesions comprised 24 FNHs, 11 adenomas including 7 telangiectatic adenomas, 10 haemangiomas, 1

focal fatty change and 4 malignant lesions: 2 adenomas with malignant foci, 1 hepatocellular carcinoma (HCC) and 1 epithelioid haemangi endothelioma. All patients had a solitary lesion except three patients who had two liver lesions: two FNHs, two haemangiomas and one haemangioma associated with FNH. Lesions ranged from 1.4 to 12 cm in diameter (mean 4.8 cm).

Pathological confirmation of the diagnosis was obtained when the diagnosis remained uncertain after complete imaging evaluation (US, CT and MR imaging) in 25 of the 50 (50%) lesions by liver biopsy ( $n=16$ ) or surgery ( $n=9$ ): 9 FNH, 11 adenomas, 1 haemangioma, and all 4 malignant tumours. The 25 lesions that were not confirmed histologically were 15 FNHs, 9 haemangiomas and 1 focal fatty change. The final diagnosis was confirmed in these 25 lesions based on a consensus interpretation of all unenhanced ultrasound, contrast-enhanced ultrasound videos, CT and MR imaging according to criteria published in the literature [2, 3, 10–12] by two experts who did not participate in the readings. Furthermore all these patients were clinically followed up for at least 1 year with imaging examination demonstrating no change over time.

### Imaging technique

Lesions were all evaluated with baseline US, contrast-enhanced US and contrast-enhanced MR imaging.

Baseline and contrast-enhanced US were performed by physicians with more than 15 years' experience in liver ultrasound and more than 4 years in contrast-enhanced ultrasound. All examinations were performed using microbubble-specific imaging. US examinations were performed with an Aplio device by pulse inversion imaging (Toshiba Medical Systems) in centre 1 and with a Sequoia device (Acuson, Siemens Medical solution) by coherent pulse sequencing (CPS)—CPS uses proper amplitude and phase combinations—in centre 2. This technology supports effective tissue signal rejection and bubble signal extraction all within the same fundamental frequency band. The US contrast agent, Sonovue (Altana-Bracco, Milan, Italy), was administered intravenously in all patients as one or two small boluses of 2.4 mL each, followed by a 10-mL saline flush. Real-time imaging was used with the imaging technique at a mechanical index of less than 0.2, which preserves the microbubble population while allowing vessels of the lesion to be evaluated and enhancement of the lesion and liver. The Aplio uses one transmit focal zone and the Sequoia uses a minimum of two focal zones. The transmit focal zone (or the upper transmit focal zone) was positioned distal to the lesion of interest. Image frame rate was 10–15 frames per second. The region of interest was observed continuously for about 3 min after injection. The arterial phase was defined as the 10- to 45-s interval after the flush was completed, the portal phase, 45 to 120 s and the late phase after 120 s. US Images were recorded in avi files.

In both centres, MR imaging was performed with a 1.5-T MR system (Intera, Philips Medical system, Eindhoven, Netherlands; and Excite, GE Healthcare, Milwaukee, WI, USA) using a phased-array body coil. The standard protocol included the following sequences acquired in the axial plane: fat-suppressed T2-weighted FSE sequences; in-phase and opposed-phase GE T1-weighted sequences, three-dimensional gadolinium-enhanced GRE sequences, and a 2D delayed GRE fat-suppressed T1-weighted sequence. Detailed technical parameters are shown in Table 1. In both centres, T1-weighted fat-suppressed 3D GRE MR images were obtained immediately before and 15, 45 and 120 s after the start of bolus injection of a non-hepatospecific gadolinium-based contrast agent at a dose of 0.1 mmol per kilogram of body weight (Dotarem, Guerbet, Aulnay sous Bois, France) followed by a 20-mL bolus of saline. Gadolinium-based contrast agent and saline were injected at a rate of 2 mL/s with the power injector.

### Blind reading

Two independent, experienced radiologists (17 and 22 years of experience in MR imaging, respectively, and 8 years of experience in CEUS) randomly reviewed MR data and US cineloops off-line and on-screen. Image analysis of US included baseline data and contrast-enhanced phases. Both readers were blinded to the final diagnosis and to the patients' identity, clinical histories and other imaging findings. Randomisation helped ensure that no US scan was shown consecutively with its corresponding MR image, i.e. avoiding one imaging technique influencing the diagnosis made with the other.

Both readers filled in a questionnaire regarding each lesion and for both imaging techniques. Image readers were asked to assess the following items in each lesion on MR imaging: signal intensity in T1- and T2-weighted images,

homogeneous or heterogeneous pattern, signal drop in out-of-phase images, and the presence of a central scar, capsule or lobulated contour. Arterial enhancement was classified as diffuse homogeneous, diffuse heterogeneous, peripheral nodular or rim. The presence of washout (defined as enhancement less than that of the liver) or sustained enhancement was determined in the portal venous and delayed phases.

Readers were asked to assess the following items for each lesion on US: echogenicity of the liver on the baseline US, homogeneous or heterogeneous pattern, presence and distribution of colour/power Doppler unenhanced ultrasound flow signals. The readers were asked to note the time of enhancement in contrast-enhanced ultrasound. The contrast enhancement pattern during the arterial phases was classified as *absent* i.e. no difference in enhancement between the lesion before and the lesion after microbubble contrast agent injection; *dotted* i.e. tiny separate spots of enhancement distributed throughout the lesion; *discontinuous* i.e. nodular peripheral enhancement with centripetal filling; *central spoke-wheel-shaped* i.e. enhancement with a central vessel appearing to branch from the centre to the periphery of the lesion; and *diffuse* i.e. homogeneous or heterogeneous enhancement of the entire lesion. The presence of washout or sustained enhancement was determined in the portal venous and delayed phases.

Both readers were then asked to provide the most likely diagnosis ("histotype" diagnosis) of the liver lesion according to established criteria in the literature [2, 3, 10–19]. Table 2 shows the diagnostic criteria for the most common liver lesions at MR imaging and CEUS. The following diagnoses were proposed: haemangioma, focal nodular hyperplasia, adenoma, focal steatosis or malignant lesion.

A five-point scale was used to grade the confidence level: 5, definitely; 4, very likely; 3, likely; 2, unlikely; 1, very unlikely.

**Table 1** MR imaging sequences and parameters

MR sequence	Centre number	TR (ms)	TE (OP/IP) (ms)	Flip angle (°)	Section thickness (mm)	Intersection gap (mm)	Phase matrix × frequency matrix	Field of view (cm)
T2-weighted FSE	1	1,600	90		4	1	256×320	36–42
	2	Depending	85		6	1.2	224×416	36–48
T1-weighted Dual 2D GRE	1	236	2.2/4.4	80	5	1	160×256	36–42
	2	170	2/4.3	75	7	2.5	256×256	36–48
T1-weighted 3D GRE	1	4.9	2.4	10	4	0	256×320	36–42
	2	3.9	1.8	12	4	0	224×256	36–48
Delayed T1-weighted 2D GRE	1	212	5	80	6	2	226×320	36–42
	2	165	5	80	6	2	224×416	36–48

TR repetition time, TE echo time, FSE fast spin echo, GRE gradient echo, 3D three-dimensional, 2D two-dimensional, OP/IP out-of-phase/in-phase

**Table 2** MR and CEUS diagnostic criteria for the assessment of focal liver lesions

	T2	T1 in-phase and out-of-phase (IP-OP)	Arterial phase	Portal phase	Late phase
Malignant lesions					
HCC	Slightly hyperintense	Iso- or hypointense. Clearly hypointense at OP if fatty content	Hyperenhanced. Sometimes only weak arterial enhancement in well-differentiated tumours	Iso- or hypoenhanced, usually rapid washout	Mostly hypoenhanced. Sometimes isoenhanced in well-differentiated tumours
Cholangiocarcinoma (peripheral mass forming)	Slightly hyperintense	Iso- or hypointense	Moderately hyperenhanced. Often rim enhancement	Hypo- or isoenhanced	Late enhancement. <i>Mostly hypoenhanced</i>
Hypervascular metastasis	Hyperintense	Iso- or hypointense	Hyperenhanced. Sometimes restricted to the margin in large lesions	Iso- or hypoenhanced	Iso- or hypoenhanced. <i>Always hypoenhanced</i>
Hypovascular metastasis	Hyperintense	Iso or hypointense	Iso- or hypoenhanced. <i>Briefly hyperenhanced</i>	Hypoenhanced. <i>Iso- or hypoenhanced</i>	Iso- or hypoenhanced, sometimes late enhancement. <i>Always hypoenhanced</i>
Benign lesions					
Haemangioma	Strongly hyperintense	Hypointense	Peripheral nodular enhancement. In high-flow haemangiomas: complete filling of the lesion during arterial phase	Slow centripetal progression of the enhancement leading to an hyperenhanced appearance	More or less complete enhancement, prolonged compared with surrounding liver tissue
Focal nodular hyperplasia	Iso- or hyperintense. Central scar is more intense in typical case	Iso- or hypointense. Rarely hypointense at OP in the case of fatty HNF	Strongly hyperenhanced. <i>Fast centrifugal filling of the lesion; usually a central vessel and radial vascular branches are delineated</i>	Iso- or hyperenhanced	Iso- or hyperenhanced, central scar shows delayed enhancement in typical case. <i>Hypoenhanced central scar is rarely visible</i>
Hepatic adenoma	Variable but mostly hyperintense. Sometimes heterogeneous	Iso- or hypointense. Sometimes hypointense at OP in the case of fatty adenoma	Hyperenhanced. Sometimes heterogeneous. <i>Frequently fast filling and rapid contrast washout; no radial vascular structures but delineation of feeding vessels inside of the lesion is possible</i>	Iso-, hyper- or hypoenhanced. Sometimes heterogeneous	Iso-, hyper- or hypoenhanced, no central scar visible
Focal fatty accumulation	Slightly hyperintense. Isointense if fat-suppressed	Isointense at IP and clearly hypointense at OP	Isoenhanced	Isoenhanced	Isoenhanced
Focal fatty sparing	Slightly hypointense. Isointense if fat-suppressed	Isointense at IP and clearly hyperintense at OP	Isoenhanced	Isoenhanced	Isoenhanced

Specificities of the enhancement of CEUS during the different vascular phases are reported in italics

## Data and statistical analysis

The percentage of diagnoses made by each reader for each imaging procedure was first computed and compared using McNemar's test ( $p < 0.05$ ).

To assess the diagnostic performance of MR imaging and CEUS for characterising liver lesions, the sensitivity, specificity and likelihood ratios (LR) for positive tests (i.e. confidence levels 4 and 5) were computed. Confidence intervals (CI) for sensitivity and specificity were computed using the exact binomial formula. CIs for likelihood ratios were computed with the delta method. LR estimates and CIs were computed using a 0.5 continuity correction in the case of sampling zeros; in that case, CIs for LR were recalculated using the score method to check that continuity correction provided conservative estimates.

The LR is a convenient way to summarise the sensitivity and specificity of a diagnostic test into a single value that reflects the discriminant power of the test. Specifically, the LR of a positive test is the ratio of the probability of a positive test result in a patient with the disease being tested and in a patient without, i.e.  $LR = \text{sensitivity}/(1 - \text{specificity})$ . In practice, if a pre-test assessment of the probability ( $p_1$ ) that the investigated diagnosis is correct is made,  $p_1$  can be graphically combined with the LR to give the post-test probability ( $p_2$ ) that the diagnosis is true using a nomogram [20]. Alternatively,  $p_2$  can be computed manually because multiplying the pre-test odds of the disease by the LR gives the odds of the disease following a positive test:  $(p_1/(1 - p_1)) \times LR = p_2/(1 - p_2)$ .

A descriptive analysis of mistaken and uncertain diagnoses was made. Mistaken diagnoses were lesions classified with a confidence level of 4 or 5 but whose final diagnosis was different. Uncertain diagnoses were lesions classified with a confidence level of 3 or below. We assessed the number of additional diagnoses that each reader would have made for these lesions if he had switched to the other imaging technique.

Finally, the kappa statistic was used to assess inter-observer agreement for each technique. Reproducibility of the overall diagnosis was assessed using a separate diagnostic category for uncertain diagnoses. Corresponding confidence intervals were computed using the non-parametric bootstrap method.

Score confidence intervals [21] were computed using R 2.6 statistical software [22]. All other statistical computations were performed with SAS 9.1 (SAS Institute, Inc, Cary, NC, USA) or Stata 9.2 (Statacorp, College Station, TX, USA).

## Results

### MR imaging and CEUS performance

All MR examinations were considered satisfactory by the readers. Two CEUS examinations were considered unsa-

tisfatory by reader 1 because of movement artefacts, but only one of these examinations was considered unsatisfactory by reader 2. These examinations were not included in the assessment of CEUS because the movements occurred at random and the imaging procedure would have been repeated in a standard clinical setting [23]. The two CEUS examinations that were discarded by at least one of the readers were a haemangioma (examination discarded by both readers) and an FNH (discarded by reader 1).

A histotype diagnosis was obtained with MR imaging in 33 out of 50 lesions (66%) by reader 1 and 26 out of 50 by reader 2 (52%) ( $p = 0.034$ ). A histotype diagnosis was obtained with CEUS in 25 out of 48 lesions (52%) by reader 1 and 26 out of 49 by reader 2 (53%) (not significant [ns]).

Eight out of nine (88.9%) haemangiomas were correctly diagnosed with CEUS by both readers. One of the nine haemangiomas was classified with a confidence level below 4 by each reader because the lesion did not show peripheral globular enhancement during the arterial phase: one 1.5-cm, deep (10 cm) haemangioma was classified with a confidence level of 2 by reader 1 and one 10-cm haemangioma with a confidence level of 2 by reader 2. All haemangiomas (10/10, 100%) were correctly diagnosed at MR imaging by both readers. There were no false-positive haemangiomas with either imaging technique.

FNHs were correctly diagnosed on CEUS by reader 1 and reader 2 in 17/23 (73.9%) and 16/24 (66.7%) cases, respectively. FNHs were correctly diagnosed on MR imaging by reader 1 and reader 2 in 21/24 (87.5%) and 15/24 (62.5%), respectively (Fig. 1).

The sensitivity, specificity and likelihood ratio for diagnosing liver haemangioma and FNH for readers 1 and 2 are summarised in Table 3.

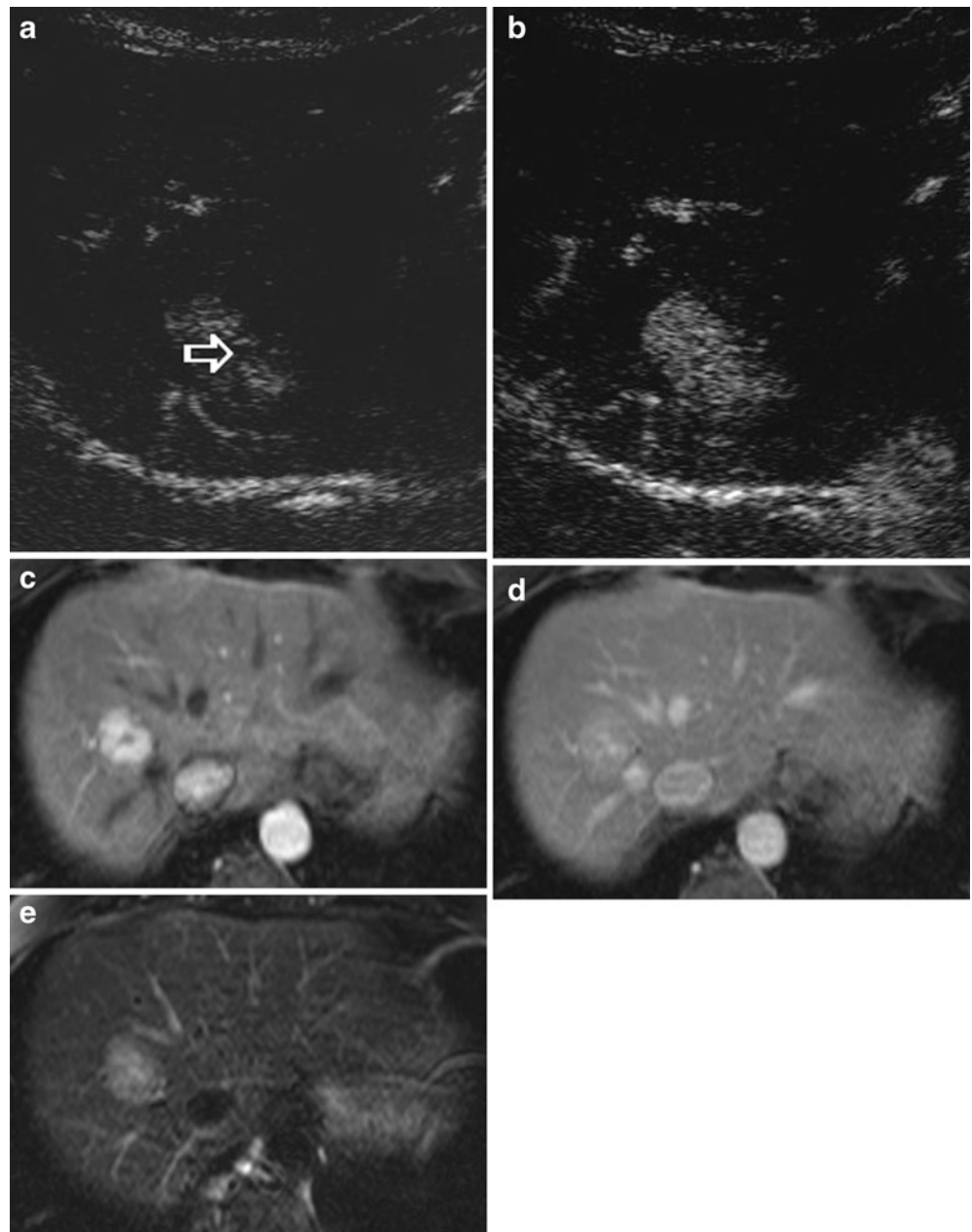
None of the adenomas was correctly diagnosed on CEUS by either reader. Two adenomas (2/11 = 18%) were correctly diagnosed by reader 1, while none was correctly diagnosed by reader 2 on MR imaging.

All malignant lesions were classified as uncertain by both readers with CEUS and MR imaging except for one HCC (1/1) which was correctly diagnosed by reader 2 with CEUS (CEUS confidence level 4; MR imaging confidence level 3).

### Mistaken diagnosis

There were six mistaken diagnoses, which are summarized in Table 4. Three adenomas were misdiagnosed as FNH with CEUS, and one with both CEUS and MR imaging. Three out of these four (75%) adenomas had a spoke-wheel artery pattern with CEUS, including one that was misdiagnosed as FNH on MR imaging (Fig. 2). These four adenomas were all telangiectatic. They were homogeneous on grey-scale ultrasound and on MR imaging. There were no imaging findings suggesting

**Fig. 1** A 50-year-old woman with FNH. CEUS showed a homogeneous lesion in the arterial phase with a visible central artery in the very early phase (a, b). MR imaging showed a lesion with homogeneous arterial enhancement (c), and a central scar best seen on delayed T1- and T2-weighted sequences (d, e). Both readers classified this lesion as definite FNH on CEUS and MR imaging



fat, haemorrhage or necrosis. All had sustained enhancement on portal and delayed phase imaging. One fatty FNH was misdiagnosed as an adenoma with MR imaging. Focal fatty change was misdiagnosed as an adenoma by MR imaging.

#### Interobserver agreement

The interobserver agreement for the diagnosis of lesions with MR imaging and CEUS was 0.68 (95% CI 0.46–0.85) and 0.58 (95% CI 0.30–0.73), respectively.

#### Contribution of the other imaging techniques in uncertain lesions

If CEUS was used as the first-line technique:

- Reader 1 classified 19 lesions as having an uncertain diagnosis (confidence degree 3 or below) in: 1 haemangioma, 6 FNHs, 8 adenomas and 4 malignant lesions. In these cases, a correct histotype diagnosis was made with a higher confidence level (4 or 5) with MR imaging in: 1/1 haemangioma, 4/6 FNHs, 2/8 adenomas and none of the four malignant lesions.

**Table 3** MR imaging and contrast-enhanced US results for the two most common solid benign lesions

	Haemangioma ( <i>n</i> =10)			FNH ( <i>n</i> =24)		
	Se	Sp	LR	Se	Sp	LR
Reader 1						
MR imaging	10/10 (100) (CI 0.69–1)	40/40 (100) (CI 0.91–1)	78.3 <sup>b</sup> (4.96–1,234) <sup>c</sup>	21/24 (87.5) (CI 0.68–0.97)	25/26 (96.2) (CI 0.8–1)	22.8 (3.31–156)
CEUS	8/9 (88.9) <sup>a</sup> (CI 0.44–0.97)	39/39 (100) <sup>a</sup> (CI 0.91–1)	68 <sup>b</sup> (4.28–1,082) <sup>d</sup>	17/23 (73.9) <sup>a</sup> (CI 0.49–0.87)	22/25 (88) <sup>a</sup> (CI 0.7–0.98)	6.16 (2.07–18.3)
Reader 2						
MR imaging	10/10 (100) (CI 0.69–1)	40/40 (100) (CI 0.91–1)	78.3 <sup>b</sup> (4.96–1,234) <sup>e</sup>	15/24 (62.5) (CI 0.41–0.81)	26/26 (100) (CI 0.87–1)	33.5 <sup>b</sup> (2.11–531) <sup>g</sup>
CEUS	8/9 (88.9) <sup>a</sup> (CI 0.44–0.97)	40/40 (100) (CI 0.91–1)	69.7 <sup>b</sup> (4.38–1,109) <sup>f</sup>	16/24 (66.7) (CI 0.45–0.84)	24/25 (96) <sup>a</sup> (CI 0.8–1)	16.7 (2.39–116)

Numbers in parentheses are percentages

Se sensitivity, Sp specificity, LR likelihood ratio, CI confidence interval

<sup>a</sup>Two CEUS examinations were discarded by reader 1: one haemangioma and one FNH; and one CEUS examination was discarded by reader 2: one FNH

<sup>b</sup>A continuity correction was applied before computation

<sup>c–g</sup>Conservative CI estimates, computed after continuity correction. CIs based on the score method are as follows ( $\infty$  symbol indicates that the upper bound is infinite): <sup>c</sup>Score CI = [11.41– $\infty$ ]; <sup>d</sup>Score CI = [9.84– $\infty$ ]; <sup>e</sup>Score CI = [11.41– $\infty$ ]; <sup>f</sup>Score CI = [10.07– $\infty$ ]; <sup>g</sup>Score CI = [4.79– $\infty$ ]

- Reader 2 classified 22 lesions as having an uncertain diagnosis (confidence degree 3 or below) in: 1 haemangioma, 8 FNHs, 10 adenomas and 3 malignant lesions. In these cases, a correct histotype diagnosis was made with a higher confidence level (4 or 5) with MR imaging in: 1/1 haemangioma, 4/8 FNHs and none of the adenomas or the 3 malignant lesions.
- Reader 2 classified 24 lesions as having an uncertain diagnosis (confidence degree 3 or below) in: 9 FNHs, 11 adenomas and the 4 malignant lesions. In these cases, a correct histotype diagnosis was made with a higher confidence level (4 or 5) with CEUS in: 5/9 FNHs, 1/4 malignant lesions (HCC) and none of the 8 adenomas.

If MR imaging was used as the first-line technique:

- Reader 1 classified 14 lesions as having an uncertain diagnosis (confidence degree 3 or below) in: 2 FNHs, 8 adenomas, and the 4 malignant lesions. In these cases, a correct histotype diagnosis was made with a higher confidence level (4 or 5) with CEUS in: 1/2 FNHs (Fig. 3) and none of the 8 adenomas and the 4 malignant lesions.

**Table 4** Mistaken diagnosis by both readers

Final diagnosis	Reader 1		Reader 2	
	MR	CEUS	MR	CEUS
FNH <sup>a</sup>	Adenoma	–	–	–
Adenoma <sup>b</sup>	–	FNH	–	–
Adenoma <sup>b</sup>	–	FNH	–	–
Adenoma <sup>b</sup>	–	–	–	FNH
Adenoma <sup>b</sup>	FNH	FNH	–	–
Focal steatosis	Adenoma	–	–	–

<sup>a</sup>This FNH contained fat on histology

<sup>b</sup>These four liver adenomas were all telangiectatic types

## Discussion

Although many studies have shown that the diagnosis of liver tumours has improved with CEUS, a prospective comparison with MR imaging in incidentally discovered liver lesions has not yet been performed. This clinical setting is important because although the probability of benign lesions is very high, malignant tumours may be found. The role of imaging is not only to assess whether a lesion is benign or malignant, it is to obtain a histotype diagnosis. In particular, specificity for the diagnosis of benign lesions should be as high as possible, to avoid the necessity of any additional testing. Our results show that CEUS had a good diagnostic value in this clinical context and provided correct histotype diagnosis in 52% of the lesions for reader 1 and in 53% of the lesions for reader 2. These results are comparable to those of MR imaging which ranged from 52% for reader 2 to 66% for reader 1. These results, which may seem somewhat disappointing, could be because only diagnoses assessed with a high level of confidence (very likely or definitely) were considered in this study. Also, this study did not compare these imaging

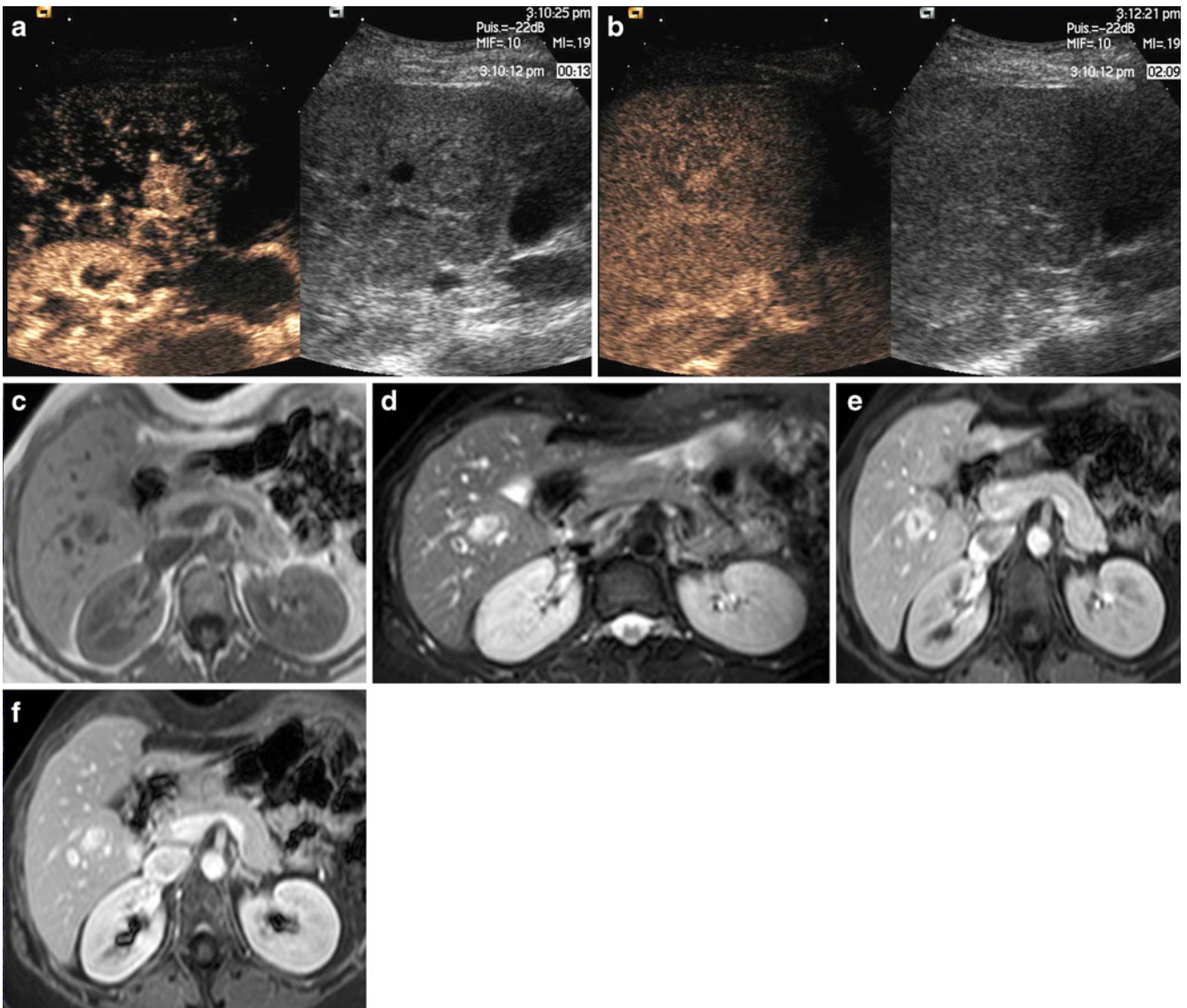


**Fig. 2** A 41-year-old woman with a telangiectatic adenoma. CEUS showed a homogeneous lesion on the arterial phase with spoke-wheel pattern (a), and isoechoic appearance in the portal venous and late phases (b). MR imaging showed a hypointense lesion on T1-

weighted image (c) and hyperintense on T2-weighted image (d) with a homogeneous arterial enhancement with a central scar (e), and sustained enhancement in the portal phase (f). This lesion was mistaken as an FNH with MR imaging and CEUS by one reader

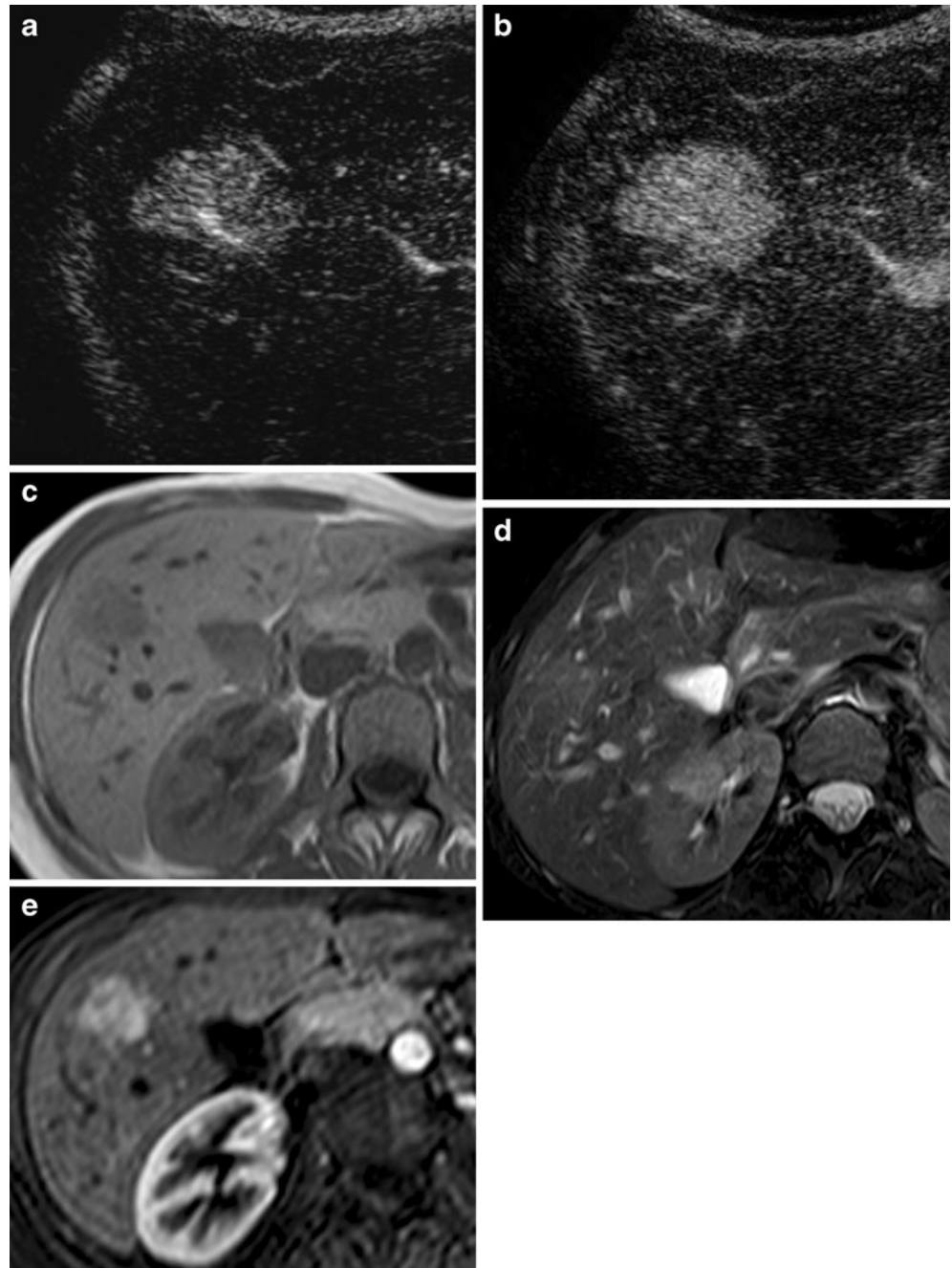
techniques in all incidental liver lesions, only in incidental focal solid liver lesions that were not characterised during routine US. This inclusion criterion explains the relatively low prevalence of haemangiomas and the high number of FHNs and hepatocellular adenomas.

In this series, both CEUS and MR imaging very accurately diagnosed haemangiomas that were not typical on grey-scale ultrasound. The sensitivity, specificity and likelihood ratios were 89%, 100% and 68–70 for CEUS, and 100%, 100% and 78.3 for MR imaging, respectively. Our results are similar to those of other authors. Youk et al. reported that CEUS had a sensitivity of 89% and a specificity of 100% in the diagnosis of haemangiomas,

while Leen et al. in 2006 showed that CEUS had a accuracy of 84–92% for the diagnosis of haemangiomas [24, 25]. This confirms that CEUS characterises haemangiomas approximately as well as MR imaging, even for small lesions. Burns et al. showed that results identifying the two hallmarks of haemangioma, peripheral puddles and pools and centripetal progression, are nearly identical on CEUS and MR imaging [26]. We also used the likelihood ratio to evaluate the performance of CEUS and MR imaging. The likelihood ratio incorporates test sensitivity and specificity and provides a direct estimate of how much a test result will change the odds of having a disease [27]. A likelihood ratio above 2 indicates a significant impact on the



**Fig. 3** A 35-year-old woman with FNH. On CEUS, a central artery is clearly visible in the centre of the lesion 15 s after injection (**a**). A few seconds later CEUS shows a homogeneous hypervascular lesion (**b**). MR imaging showed a hypointense lesion on the T1-weighted image (**c**) which looked slightly hyperintense on the T2-weighted image (**d**) with a homogeneous arterial enhancement without a visible central scar (**e**). Both readers classified this lesion as definite FNH on CEUS, but as likely FNH on MR imaging



diagnosis. In our series, the confidence intervals of the likelihood ratios were wide; however, the lower confidence interval bounds were still high, close to five for haemangiomas on both CEUS and MR imaging. Having a 100% specificity with CEUS when diagnosing haemangiomas is extremely important in clinical practice because it means that the lesion can be reliably characterised and the patient can be reassured during the examination.

The sensitivity, specificity and likelihood ratios for diagnosing FNH with CEUS were 67–74%, 88–96% and 6–17, respectively, while they were 63–88%, 96–100% and

23–34 with MR imaging. Both imaging techniques had confidence interval lower bounds of likelihood ratio superior to 2. Our results are close to those in the literature [3, 26], especially those of a study by Leen et al. that showed that the accuracy of CEUS for the diagnosis of FNH was 77–85% [25]. Recently, another study determined the differentiating features of FNH and hepatic adenoma in CEUS and showed a sensitivity ranging from 86 to 95% and a specificity from 74 to 79% [16]. Differences between that study and ours might be because the former focused on FNH and hepatocellular adenoma.

Interestingly, although the sensitivities were higher than ours, the specificities were lower. Again, it is important to stress that higher specificity is preferable to higher sensitivity for benign lesions.

In our study, the false-positive cases of FNH using CEUS were only hepatocellular adenomas and never malignant tumours. It is interesting to note that these false-positives were all telangiectatic adenomas. These lesions were previously called “telangiectatic focal nodular hyperplasia” [28, 29] but they were recently reclassified as “telangiectatic adenoma” based on molecular evidence including clonal analysis and gene expression studies [30]. Therefore, it is not surprising that this lesion—which is at the limit of FNH and adenoma—was misdiagnosed with CEUS. In particular, three out of the four telangiectatic adenomas misdiagnosed as FNH had a spoke-wheel pattern and all had sustained enhancement.

Unlike for haemangiomas and FNHs, both CEUS and MR imaging were of limited value in diagnosing hepatocellular adenomas with a high level of confidence in this series. This is not surprising because there is no specific vascular pattern in hepatocellular adenomas [15]. Kim and colleagues reported that the most common findings on CEUS were centripetal or mixed filling (84%) and sustained portal phase enhancement (47% and 63%) [16]. However, in their experience, prediction of hepatocellular adenomas was less reliable than FNH [16].

We have also shown that MR imaging and CEUS are complementary imaging techniques. When diagnosis of haemangioma was uncertain with CEUS, MR imaging always confirmed the diagnosis. When diagnosis of FNH was uncertain with either CEUS or MR imaging, the other imaging technique confirmed the diagnosis in approximately half the cases. This raises the question of the first choice imaging technique in incompletely characterised, solid liver lesions detected during routine US. CEUS seems to be a reasonable choice for the first intention because it is rapid and could significantly reduce both costly diagnostic tests and patient waiting time. A recent Italian multicentric study showed that the routine use of CEUS for the characterisation of focal liver lesions provides significant cost savings [31]. An important issue in this case is

interobserver agreement. Although Leen and co-workers found significant interobserver variability with CEUS, our results showed that the interobserver agreement with CEUS and MR imaging were good: 0.58 and 0.68, respectively [25]. The difference between the two imaging methods might be because MR imaging is the reference method for the characterisation of benign liver tumours with well-known and established criteria [10, 11, 32, 33]. CEUS is a more innovative technique with criteria that have evolved over time.

Our study has several limitations. First, our patient population was limited with only 50 lesions, although it was a prospective and bicentric study, using the same CEUS and MR imaging protocols in both centres with blind off-site readings. Second, final diagnoses were not all histologically proven and in those cases, combined imaging was used as the reference method for the final diagnosis which was made after a consensus interpretation of all examinations by two experts who did not participate in the readings. Yet if we had only considered lesions that had been histologically confirmed, we would have introduced a huge bias into the patient population because only a few benign liver lesions undergo liver biopsy and our conclusions would not have been applicable to the usual population of incidental liver lesions. Moreover, the only lesions that were not biopsied were haemangiomas and FNHs whose specificities achieve 100% with imaging [32, 33]. Third, we attempted a histotype characterisation of the lesions instead of a nature characterisation (benign vs. malignant). We think that specific diagnosis is crucial because it reflects the general management of benign liver lesions. While haemangiomas do not require any follow-up, most centres usually follow-up FNH for at least a year. Conversely, liver adenomas which are benign hepatocellular lesions like FNHs usually require surgical resection [34, 35].

In conclusion, this study shows that both CEUS and non-hepatospecific MR imaging accurately diagnose most incidental solid liver lesions (haemangiomas and FNHs) detected on routine US but not completely characterised. Therefore, we suggest that CEUS should be the first-line imaging technique in these cases and that MR imaging is indicated if in doubt.

## References

1. Little JM, Richardson A, Tait N (1991) Hepatic dystychoma: a five year experience. *HPB Surg* 4:291–297
2. Semelka RC, Sofka CM (1997) Hepatic hemangiomas. *Magn Reson Imaging Clin N Am* 5:241–253
3. Vilgrain V (2006) Focal nodular hyperplasia. *Eur J Radiol* 58:236–245
4. Quaia E, Stacul F, Gaiani S, Ricci P, Passariello R, Curzio D et al (2004) Comparison of diagnostic performance of unenhanced vs SonoVue - enhanced ultrasonography in focal liver lesions characterization. The experience of three Italian centers. *Radiol Med (Torino)* 108:71–81
5. Nicolau C, Vilana R, Catala V, Bianchi L, Gilibert R, Garcia A et al (2006) Importance of evaluating all vascular phases on contrast-enhanced sonography in the differentiation of benign from malignant focal liver lesions. *AJR Am J Roentgenol* 186:158–167

6. Albrecht T, Blomley M, Bolondi L, Claudon M, Correas JM, Cosgrove D et al (2004) Guidelines for the use of contrast agents in ultrasound. *January 2004. Ultraschall Med* 25:249–256
7. Claudon M, Cosgrove D, Albrecht T, Bolondi L, Bosio M, Calliada F et al (2008) Guidelines and good clinical practice recommendations for contrast enhanced ultrasound (CEUS) - update 2008. *Ultraschall Med* 29:28–44
8. Elsayes KM, Leyendecker JR, Menias CO et al (2007) MRI characterization of 124 CT-indeterminate focal hepatic lesions: evaluation of clinical utility. *HPB (Oxford)* 9:208–215
9. Phongkitkarun S, Sriarujata T, Jatchavala J (2009) Supplement value of magnetic resonance imaging in small hepatic lesion (< or = 20 mm) detected on routine computed tomography. *J Med Assoc Thai* 92:677–686
10. Vilgrain V, Flejou JF, Arrive L, Belghiti J, Najmark D, Menu Y et al (1992) Focal nodular hyperplasia of the liver: MR imaging and pathologic correlation in 37 patients. *Radiology* 184:699–703
11. Soyer P, Gueye C, Somveille E, Laissy JP, Scherrer A (1995) MR diagnosis of hepatic metastases from neuroendocrine tumors versus hemangiomas: relative merits of dynamic gadolinium chelate-enhanced gradient-recalled echo and unenhanced spin-echo images. *AJR Am J Roentgenol* 165:1407–1413
12. Buetow PC, Pantongrag-Brown L, Buck JL, Ros PR, Goodman ZD (1996) Focal nodular hyperplasia of the liver: radiologic-pathologic correlation. *Radiographics* 16:369–388
13. Horton KM, Bluemke DA, Hruban RH, Soyer P, Fishman EK (1999) CT and MR imaging of benign hepatic and biliary tumors. *Radiographics* 19:431–451
14. Arrive L, Flejou JF, Vilgrain V, Belghiti J, Najmark D, Zins M et al (1994) Hepatic adenoma: MR findings in 51 pathologically proved lesions. *Radiology* 193:507–512
15. Quaia E, Calliada F, Bertolotto M, Rossi S, Garioni L, Rosa L et al (2004) Characterization of focal liver lesions with contrast-specific US modes and a sulfur hexafluoride-filled microbubble contrast agent: diagnostic performance and confidence. *Radiology* 232:420–430
16. Kim TK, Jang HJ, Burns PN, Murphy-Lavallee J, Wilson SR (2008) Focal nodular hyperplasia and hepatic adenoma: differentiation with low-mechanical-index contrast-enhanced sonography. *AJR Am J Roentgenol* 190:58–66
17. Wilson SR, Burns PN (2006) An algorithm for the diagnosis of focal liver masses using microbubble contrast-enhanced pulse-inversion sonography. *AJR Am J Roentgenol* 86:1401–1412
18. Harvey CJ, Albrecht T (2001) Ultrasound of focal liver lesions. *Eur Radiol* 11:1578–1593
19. Trillaud H, Bruel JM, Valette PJ et al (2009) Characterization of focal liver lesions with SonoVue-enhanced sonography: international multicenter-study in comparison to CT and MRI. *World J Gastroenterol* 15:3748–3756
20. Fagan TJ (1975) Letter: Nomogram for Bayes theorem. *N Engl J Med* 293:257
21. Agresti A (2002) *Categorical data analysis*, 2nd edn. Wiley, New York
22. Ihaka R, Gentleman R (1996) R: a language for data analysis and graphics. *J Comp GraphStat* 5:299–314
23. Begg CB, Greenes RA, Iglewicz B (1986) The influence of uninterpretable on the assessment of diagnostic tests. *J Chronic Dis* 39:575–584
24. Youk JH, Kim CS, Lee JM (2003) Contrast-enhanced agent detection imaging: value in the characterization of focal hepatic lesions. *J Ultrasound Med* 22:897–910
25. Leen E, Ceccotti P, Kalogeropoulou C, Angerson WJ, Moug SJ, Horgan PG (2006) Prospective multicenter trial evaluating a novel method of characterizing focal liver lesions using contrast-enhanced sonography. *AJR Am J Roentgenol* 186:1551–1559
26. Burns PN, Wilson SR (2007) Focal liver masses: enhancement patterns on contrast-enhanced images—concordance of US scans with CT scans and MR images. *Radiology* 242:162–174
27. Jaeschke R, Guyatt GH, Sackett DL (1994) *Users' guides to the medical literature. III. How to use an article about a diagnostic test. B. What are the results and will they help me in caring for my patients? The Evidence-Based Medicine Working Group. JAMA* 271:703–707
28. Nguyen BN, Flejou JF, Terris B, Belghiti J, Degott C (1999) Focal nodular hyperplasia of the liver: a comprehensive pathologic study of 305 lesions and recognition of new histologic forms. *Am J Surg Pathol* 3 (12):1441–1454
29. Attal P, Vilgrain V, Brancatelli G, Paradis V, Terris B, Belghiti J et al (2003) Telangiectatic focal nodular hyperplasia: US, CT, and MR imaging findings with histopathologic correlation in 13 cases. *Radiology* 228:465–472
30. Paradis V, Champault A, Ronot M, Deschamps L, Valla DC, Vidaud D et al (2007) Telangiectatic adenoma: an entity associated with increased body mass index and inflammation. *Hepatology* 46:140–146
31. Romanini L, Passamonti M, Aiani L, Cabassa P, Raieli G, Montermini I et al (2007) Economic assessment of contrast-enhanced ultrasonography for evaluation of focal liver lesions: a multicentre Italian experience. *Eur Radiol* 17(Suppl 6):F99–F106
32. Cherqui D, Rahmouni A, Charlotte F, Boulahdour H, Metreau JM, Meignan M et al (1995) Management of focal nodular hyperplasia and hepatocellular adenoma in young women: a series of 41 patients with clinical, radiological, and pathological correlations. *Hepatology* 22:1674–1681
33. Semelka RC, Brown ED, Ascher SM, Patt RH, Bagley AS, Li W et al (1994) Hepatic hemangiomas: a multi-institutional study of appearance on T2-weighted and serial gadolinium-enhanced gradient-echo MR images. *Radiology* 192:401–406
34. Herman P, Pugliese V, Machado MA et al (2000) Hepatic adenoma and focal nodular hyperplasia: differential diagnosis and treatment. *World J Surg* 24:372–376
35. Choi BY, Nguyen MH (2005) The diagnosis and management of benign hepatic tumors. *J Clin Gastroenterol* 39:401–412